

Stabilization of an elusive tautomer by metal coordination

Emmanuele Parisi and Roberto Centore*

Dipartimento di Scienze Chimiche, Università degli Studi di Napoli 'Federico II', Complesso di Monte S. Angelo, Via Cinthia, 80126 Napoli, Italy. *Correspondence e-mail: roberto.centore@unina.it

Received 27 April 2021

Accepted 16 June 2021

Edited by D. R. Turner, University of Monash, Australia

Keywords: heterocycle; triazole; tautomerism; elusive tautomer; crystal structure; zinc; copper.

CCDC references: 2090148; 2090147

Supporting information: this article has supporting information at journals.iucr.org/c

The solid-state isolation of the different tautomers of a chemical compound can be a challenging problem. In many cases, tautomers with an energy very close to the most stable one cannot be isolated (elusive tautomers). In this article, with reference to the 4-methyl-7-(pyrazin-2-yl)-2*H*-[1,2,4]triazolo[3,2-*c*][1,2,4]triazole ligand, for which the elusive 3*H*-tautomer has an energy only 1.4 kcal mol⁻¹ greater than the most stable 2*H* form, we show that metal complexation is a successful and reliable way for stabilizing the elusive tautomer. We have prepared two complexes of the neutral ligand with CuBr₂ and ZnBr₂, namely, aquabromidobis[4-methyl-7-(pyrazin-2-yl)-3*H*-[1,2,4]triazolo[3,2-*c*][1,2,4]triazole]-copper(II) bromide trihydrate, [CuBr(C₈H₇N₇)₂(H₂O)]Br·3H₂O, and dibromido[4-methyl-7-(pyrazin-2-yl)-2*H*-[1,2,4]triazolo[3,2-*c*][1,2,4]triazole][4-methyl-7-(pyrazin-2-yl)-3*H*-[1,2,4]triazolo[3,2-*c*][1,2,4]triazole]zinc(II) monohydrate, [ZnBr₂(C₈H₇N₇)₂]·H₂O. The X-ray analysis shows that, in both cases, the elusive 3*H*-tautomer is present. The results of the crystallographic analysis of the two complexes reflect the different coordination preferences of Cu^{II} and Zn^{II}. The copper(II) complex is homotautomeric as it only contains the elusive 3*H*-tautomer of the ligand. The complex can be described as octahedral with tetragonal distortion. Two 3*H*-triazolotriazole ligands are bis-chelated in the equatorial plane, while a water molecule and a bromide ion in elongated axial positions complete the coordination environment. The zinc(II) complex, on the other hand, is heterotautomeric and contains two bromide ions and two monodentate ligand molecules, one in the 2*H*-tautomeric form and the other in the 3*H*-tautomeric form, both coordinated to the metal in tetrahedral geometry. The observation of mixed-tautomer complexes is unprecedented for neutral ligands. The analysis of the X-ray molecular structures of the two complexes allows the deduction of possible rules for a rational design of mixed-tautomer complexes.

1. Introduction

Tautomers are structural isomers in ready equilibrium between each other (McNaught & Wilkinson, 1997). They are intriguing chemical systems that, in a certain sense, can be considered as 'living molecules'. In fact, because of the equilibrium they undergo, the relative amounts of the different forms in solution can be altered by physical or chemical factors (temperature, solvent, pH, metal ions, *etc.*) through the laws of chemical equilibrium. Tautomers have been central in chemistry since the early work of Berzelius on cyanic and cyanuric acids in 1832, and the discovery of keto–enol tautomerism by Erlenmeyer in 1880 (Taylor *et al.*, 2014). The issue of tautomerism has been fundamental in many turning points of research in chemistry. For instance, it was fundamental in the discovery of the structure of DNA by Watson & Crick (1953*a*), which relies on the keto-tautomeric forms of purine and pyrimidine bases, and in their seminal hypothesis (Watson & Crick, 1953*b*) that noncanonical tautomeric forms of the

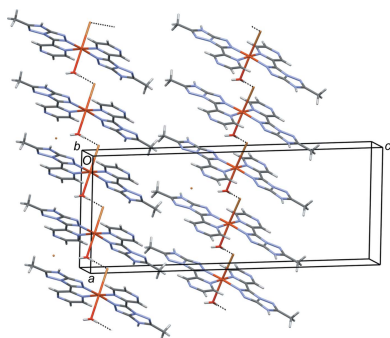


Table 1
Experimental details.

Experiments were carried out with Mo $K\alpha$ radiation using a Bruker–Nonius KappaCCD diffractometer. Absorption was corrected for by multi-scan methods (SADABS; Bruker, 2001). H atoms were treated by a mixture of independent and constrained refinement.

	1	2
Crystal data		
Chemical formula	[CuBr(C ₈ H ₇ N ₇) ₂ (H ₂ O)]Br·3H ₂ O	[ZnBr ₂ (C ₈ H ₇ N ₇) ₂ ·H ₂ O
M_r	697.83	645.62
Crystal system, space group	Monoclinic, Cc	Triclinic, $P\bar{1}$
Temperature (K)	173	293
a, b, c (Å)	11.062 (4), 8.369 (3), 27.406 (6)	8.396 (2), 12.305 (3), 12.724 (3)
α, β, γ (°)	90, 92.44 (3), 90	112.53 (2), 107.78 (3), 92.16 (2)
V (Å ³)	2534.9 (14)	1138.1 (5)
Z	4	2
μ (mm ⁻¹)	4.07	4.63
Crystal size (mm)	0.50 × 0.20 × 0.20	0.40 × 0.30 × 0.20
Data collection		
T_{\min}, T_{\max}	0.250, 0.478	0.270, 0.433
No. of measured, independent and observed [$I > 2\sigma(I)$] reflections	8682, 4870, 4563	12306, 5090, 3636
R_{int}	0.036	0.042
($\sin \theta/\lambda$) _{max} (Å ⁻¹)	0.651	0.649
Refinement		
$R[F^2 > 2\sigma(F^2)], wR(F^2), S$	0.033, 0.081, 1.04	0.047, 0.136, 1.09
No. of reflections	4870	5090
No. of parameters	367	315
No. of restraints	13	2
$\Delta\rho_{\text{max}}, \Delta\rho_{\text{min}}$ (e Å ⁻³)	0.60, -0.86	0.70, -0.74
Absolute structure	Refined as an inversion twin	–
Absolute structure parameter	0.502 (12)	–

Computer programs: COLLECT (Nonius, 1999), DIRAX/LSQ (Duisenberg *et al.*, 2000), EVALCCD (Duisenberg *et al.*, 2003), SIR97 (Altomare *et al.*, 1999), SHELXL2016 (Sheldrick, 2015), ORTEP-3 for Windows (Farrugia, 2012), Mercury (Macrae *et al.*, 2020) and WinGX (Farrugia, 2012).

bases could be involved in mutagenesis (Goodman, 1995; Wang *et al.*, 2011). Now the relevance of tautomers is increasingly recognized in many fields of applied chemistry, including drug design (Martin, 2009) and materials chemistry (Bussetti *et al.*, 2014; Horiuchi *et al.*, 2017). In the realm of coordination chemistry, tautomerism can also be a relevant issue, because some classes of ligands show tautomerism. As an example, keto–enol tautomerism is shown in amino-naphthol derivatives (Deneva *et al.*, 2019), in dihydroxy-quinolines (Todorov *et al.*, 2012) and in aroylhydrazine ligands (Borbone *et al.*, 2004), while thione–thiol tautomerism is present in dithiocarbamate ligands (Takjoo & Centore, 2013). In most of these cases, the common feature is that only one tautomeric form acts as the ligand and is found in the complexes.

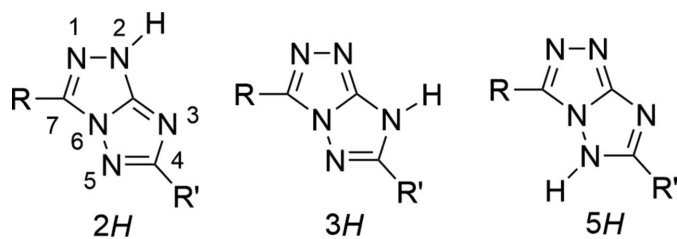


Figure 1
Relevant chemical diagrams for the [1,2,4]triazolo[3,2-*c*][1,2,4]triazole system: the three tautomers of the neutral form (the adopted atom numbering of the heterobicycle is indicated only for the 2*H*-tautomer).

In the realm of fused-ring heteroaromatic systems that we have studied over the years (Centore *et al.*, 1996, 1999; Ambrosanio *et al.*, 1999), we have found in [1,2,4]triazolo[3,2-*c*][1,2,4]triazole a heterocyclic system with a rich tautomeric behaviour (Centore *et al.*, 2013, 2015, 2017; Fusco *et al.*, 2018).

We have found that the relative energy of the three tautomers of the neutral molecule (Fig. 1) can be significantly modulated by acting on the electronic character of the substituents and on the polarity of the solvent. In all the cases investigated, the energy trend of the tautomers is $E(2H) < E(3H) \ll E(5H)$; in particular, while the predicted energy of the 5*H*-tautomer is always prohibitive (+10.8 kcal mol⁻¹ with

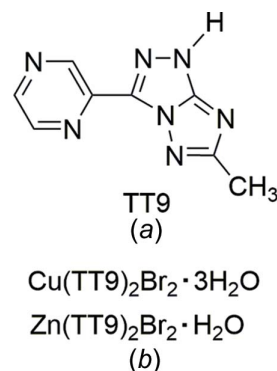


Figure 2
(a) Chemical diagram of the triazolotriazole ligand TT9 discussed in this article (the 2*H*-tautomer is shown). (b) The chemical formulae of the complexes studied in this article.

respect to the *2H*-tautomer, in the most favourable case) (Centore *et al.*, 2015), the calculated energy of the *3H*-tautomer, in some cases, is greater than for the *2H*-tautomer by only 1 kcal mol⁻¹ or less (Centore *et al.*, 2015). Despite this, the *3H*-tautomer should be considered elusive, because it has not yet been observed in the solid state for any of the pure triazolotriazole compounds studied so far.

We have recently described a new versatile nitrogen-rich triazolotriazole ligand, 4-methyl-7-(pyrazin-2-yl)-*2H,3H*-[1,2,4]triazolo[3,2-*c*][1,2,4]triazole, henceforth TT9 (Fig. 2*a*), whose tautomeric behaviour is further enriched by the possibility of metal coordination (Parisi *et al.*, 2020).

In particular, while crystallization of the pure neutral ligand yielded the most stable *2H*-tautomer, as expected, crystallization of neutral TT9 in the presence of Zn^{II} and Cu^{II} salts yielded metal complexes of the neutral ligand, with a 1:1 metal-to-ligand ratio, in which the *3H*-tautomer is present (Parisi *et al.*, 2020). In order to further confirm metal complexation as a way of stabilizing the elusive *3H*-tautomer, we report, in this article, structural data for the Zn^{II} and Cu^{II} complexes of TT9, with a 1:2 metal-to-ligand ratio (Fig. 2*b*).

2. Experimental

All reagents were of analytical grade and were used without further purification.

2.1. Synthesis and crystallization

The synthesis of the TT9 ligand was performed according to the procedure already described by us (Parisi *et al.*, 2020). Prismatic green crystals of the complex Cu(TT9)₂Br₂·3H₂O, henceforth complex **1**, were grown in 2 d by slow evaporation of a clear 50:50 (*v/v*) water–ethanol solution containing a 1:2 molar ratio of CuBr₂ dihydrate (13.0 mg, 7.63 × 10⁻⁵ mol) and TT9 (31.0 mg, 1.56 × 10⁻⁴ mol) at room temperature in a quantitative yield (53.0 mg). Prismatic brown crystals of the complex Zn(TT9)₂Br₂·H₂O, henceforth complex **2**, were grown in a week by slow evaporation of a 50:50 (*v/v*) water–ethanol solution containing a 1:2 molar ratio of ZnBr₂ (14 mg,

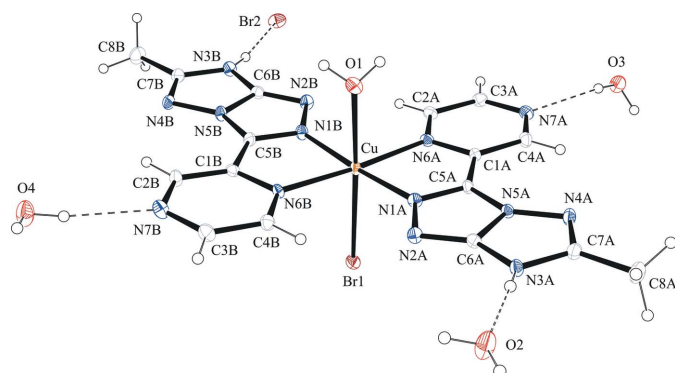


Figure 3

The molecular structure of complex **1**, with displacement ellipsoids drawn at the 30% probability level. Selected hydrogen bonds are indicated by dashed lines.

Table 2

Hydrogen-bond geometry (Å, °) for **1**.

<i>D</i> —H··· <i>A</i>	<i>D</i> —H	H··· <i>A</i>	<i>D</i> ··· <i>A</i>	<i>D</i> —H··· <i>A</i>
C2A—H2A···N2B	0.95	2.38	3.137 (8)	137
C3A—H3A···Br1 ⁱ	0.95	3.11	4.058 (6)	173
N3A—H3NA···O2	0.86 (3)	1.82 (3)	2.657 (7)	165 (7)
C4B—H4B···N2A	0.95	2.52	3.276 (8)	136
C4B—H4B···Br1 ⁱⁱ	0.95	3.09	3.848 (6)	138
N3B—H3NB···Br2	0.85 (3)	2.34 (3)	3.190 (5)	173 (7)
O1—H1W···Br1 ⁱⁱⁱ	0.83 (3)	2.42 (3)	3.229 (5)	166 (6)
O1—H2W···Br2 ⁱⁱ	0.83 (3)	2.49 (3)	3.301 (5)	168 (8)
O2—H3W···Br1 ⁱⁱ	0.82 (3)	2.43 (3)	3.237 (5)	173 (9)
O2—H4W···O3 ^{iv}	0.81 (3)	1.89 (4)	2.691 (7)	167 (10)
O3—H5W···O4 ^v	0.79 (3)	2.08 (6)	2.746 (7)	141 (8)
O3—H6W···N7A	0.80 (3)	2.17 (4)	2.931 (7)	159 (9)
O4—H7W···N7B	0.83 (3)	2.12 (3)	2.939 (7)	171 (9)
O4—H8W···Br2 ^{iv}	0.81 (3)	2.56 (6)	3.272 (6)	147 (8)

Symmetry codes: (i) $x, y - 1, z$; (ii) $x + \frac{1}{2}, y + \frac{1}{2}, z$; (iii) $x + \frac{1}{2}, y - \frac{1}{2}, z$; (iv) $x + \frac{1}{2}, y + \frac{1}{2}, z$; (v) $x, -y + 1, z + \frac{1}{2}$.

0.1 mmol) and TT9 (40 mg, 0.2 mmol) at room temperature in a 75% yield (48 mg).

2.2. Refinement

Crystal data, data collection and structure refinement details are summarized in Table 1. H atoms bonded to C atoms were generated stereochemically and refined by the riding model. After having placed C-bound H atoms, those bonded to O and N atoms, that are essential in the identification of tautomers, were clearly found in difference Fourier maps as the first maxima and, in some cases, their coordinates were refined. For all H atoms, $U_{\text{iso}}(\text{H}) = 1.2U_{\text{eq}}$ of the carrier atom was assumed (1.5 in the case of methyl groups). The structure of complex **1**, in the noncentrosymmetric space group *Cc*, was refined as a two-component inversion twin.

3. Results and discussion

The X-ray molecular structure of complex **1** is shown in Fig. 3. Two *3H*-tautomeric *s-cis* TT9 neutral ligands are coordinated to copper(II) as bidentate chelates (N1 and N6) in a square-planar arrangement, with the formation of pentatomic chelate rings. The four metal-to-ligand distances in the equatorial plane show a clear and significant asymmetry. In fact, the bond lengths with N-pyrazinic donors [Cu—N6A = 2.117 (5) and Cu—N6B = 2.125 (5) Å] are longer than with N-triazole donors [Cu—N1A = 1.953 (5) and Cu—N1B = 1.951 (5) Å]. This presumably reflects the fact that the pyrazine N atom is a poorer donor. One water molecule and one bromide ion complete the coordination environment of Cu^{II}, with *trans*-elongated bond lengths of Cu—O = 2.410 (5) and Cu—Br = 2.7466 (12) Å. The coordination geometry can be described as octahedral with tetragonal distortion. The observed coordination geometry is typical of Cu^{II} and can be related to Jahn–Teller distortions (Cotton *et al.*, 1999).

The selection of the *3H*-tautomer, in complex **1**, is probably related to the strong preference of Cu^{II} for square-planar coordination with N-donor atoms. The formation of penta-

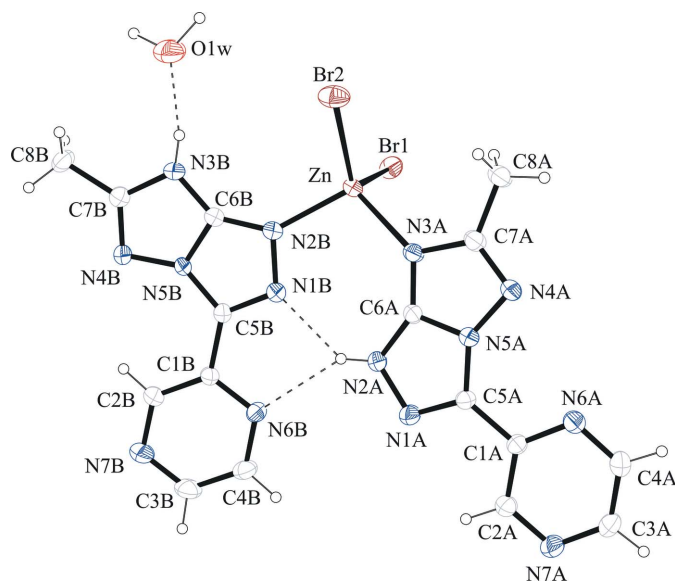


Figure 4
The molecular structure of complex **2**, with displacement ellipsoids drawn at the 30% probability level. Selected hydrogen bonds are indicated by dashed lines.

tomic (N1 and N6) chelate rings drives the selection of the *s-cis* conformer and the switching of the proton from N2 to N3. In fact, in the observed molecular structure, there are close intramolecular contacts (weak hydrogen bonds) C2A–H2A···N2B and C4B–H4B···N2A (Table 2). Three uncoordinated water molecules and a bromide ion are also present in the crystallographically independent unit. They are involved in strong hydrogen bonds with the N–H donors and N-atom acceptors present on the rim of the coordinated ligands (Table 2).

The X-ray molecular structure of complex **2**, shown in Fig. 4, has completely different features. The coordination around Zn^{II} is basically tetrahedral and is accomplished through two bromide ions [Zn–Br1 2.4017 (11) and Zn–Br2

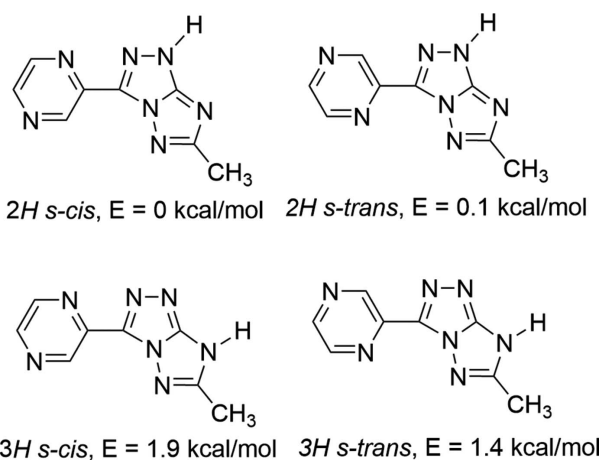


Figure 5
Low-energy tautomers/conformers of TT9. Relative energies are taken from Parisi *et al.* (2020) and are evaluated in water as the continuum polarizable medium.

Table 3
Hydrogen-bond geometry (Å, °) for **2**.

D–H···A	D–H	H···A	D···A	D–H···A
C2A–H2A···Br1 ⁱ	0.93	3.13	3.995 (6)	155
N2A–H2NA···N1B	0.84 (2)	2.09 (4)	2.786 (6)	139 (5)
N2A–H2NA···N6B	0.84 (2)	2.39 (4)	3.126 (6)	145 (5)
C2B–H2B···N4B	0.93	2.62	3.276 (7)	129
C4B–H4B···Br1 ⁱ	0.93	2.86	3.791 (6)	176
N3B–H3NB···O1W	0.85 (2)	1.85 (3)	2.669 (6)	163 (6)
O1W–H1W···Br1 ⁱⁱ	1.03	2.39	3.375 (6)	162
O1W–H2W···N7A ⁱⁱⁱ	0.98	2.03	2.901 (7)	148

Symmetry codes: (i) $-x + 1, -y, -z + 1$; (ii) $-x, -y + 1, -z + 1$; (iii) $x - 1, y + 1, z$.

2.3581 (9) Å] and two TT9 ligands acting in a monodentate manner [Zn–N3A = 2.059 (4) and Zn–N2B = 2.018 (4) Å]. The two TT9 ligands are present in different tautomer/conformers. Ligand *A* is 2*H*-tautomeric *s-trans*, whereas ligand *B* is 3*H*-tautomeric *s-cis*. In the complex, the two ligands are hydrogen bonded to each other through a strong bifurcated hydrogen bond, N2A–H2NA···N1B and N2A–H2NA···N6B (Table 3). Examples of complexes in which two different tautomeric forms of the same ligand are coordinated to the same metal centre are rare for anionic ligands (Sutradhar *et al.*, 2016), and, to the best of our knowledge, not previously documented for neutral ligands.

A deep inspection of the structure of complex **2** can suggest some basic points for the rational design of such mixed-tautomeric-ligand complexes. The two tautomeric forms should have similar ligand-donor capability and similar energy, in such a way that both are present in solution in similar amounts. They should possess complementary functional groups to form stable adducts by secondary interactions (*e.g.* hydrogen bonds), with a strong preference for mixed adducts. Finally, the mixed hydrogen-bonded adduct should be featured with a pocket, suitable for the dimensions and presence of donor atoms, to bind a metal ion. The fulfilment of all these issues may account for the rarity of the phenomenon.

The tautomeric/conformational variability of the TT9 ligand, which possesses four different tautomers/conformers within a narrow energy range $\Delta E < 2$ kcal mol⁻¹ (Parisi *et al.*, 2020), makes TT9 a reliable candidate for this target. In fact, we have considered the formation of hydrogen-bonded dimers for the four lowest-energy tautomers/conformers of TT9, shown in Fig. 5 (Parisi *et al.*, 2020). Our analysis showed that, of the ten possible combinations, only in four cases can hydrogen-bonded dimers be formed, and they are shown in Fig. 6. In all the dimers, a strong (bifurcated) hydrogen bond is present between the N–H donor of a tautomer and the two *s-cis* N-acceptor atoms of the other. The hydrogen-bonded dimers also show a pocket with two N-donor atoms that could host a metal ion, for instance, in tetrahedral coordination geometry. Of the four possible dimers, two are homo-tautomeric and contain the higher-energy 3*H*-tautomer, while the other two are heterotautomeric and contain both 2*H*- and 3*H*-tautomers. Evidently, the two latter, 2*H s-trans*/3*H s-cis* and 2*H s-cis*/3*H s-cis*, are energetically more feasible and their energies should be very close, within 0.1 kcal mol⁻¹.

Thus, our analysis confirms that the formation of mixed-tautomer complexes can be expected with TT9.

3.1. Supramolecular features

The crystal packing of both complexes is basically driven by the formation of a network of strong hydrogen bonds involving N–H donors and N-atom acceptors of the ligand molecules, the bromide ions and the water molecules (see Tables 2 and 3).

The equatorial plane of complex **1** is neither perpendicular nor parallel to the unique *b* axis. Therefore, in the crystal, molecules with two different orientations are present. The most remarkable supramolecular architecture is represented by hydrogen-bonded chains running along *a*–*b* and *a*+*b* (Fig. 7); these directions are equivalent by symmetry in the monoclinic system through the *c*-glide operation perpendicular to the unique *b* axis. The chains are formed by hydrogen bonding between water donors and bromide acceptors axially coordinated to the metal in consecutive complex molecules along the chains. Different chains are held together laterally by hydrogen bonds involving noncoordinated water molecules.

In complex **2**, an intramolecular bifurcated hydrogen-bonding interaction is present between the N2A–H2NA donor group and the N1B and N6B acceptors of the two coordinated ligands. The most remarkable supramolecular architecture is represented by nearly planar hydrogen-bonded ribbons of molecules, running along *a*–*b*. The ribbons contain

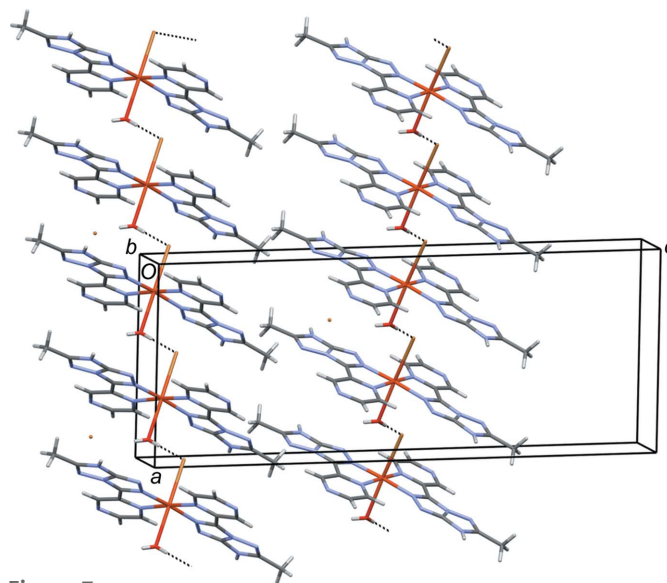


Figure 7
Partial crystal packing of complex **1**. Selected hydrogen bonds are indicated by dashed lines.

2*H*-tautomeric *s*–*trans* and 3*H*-tautomeric *s*–*cis* ligand molecules intercalated by water molecules (Fig. 8).

4. Conclusions

Nitrogen-rich ligand TT9, *i.e.* 4-methyl-7-(pyrazin-2-yl)-2*H*-[1,2,4]triazolo[3,2-*c*][1,2,4]triazole, has a low-energy 3*H*-tauto-

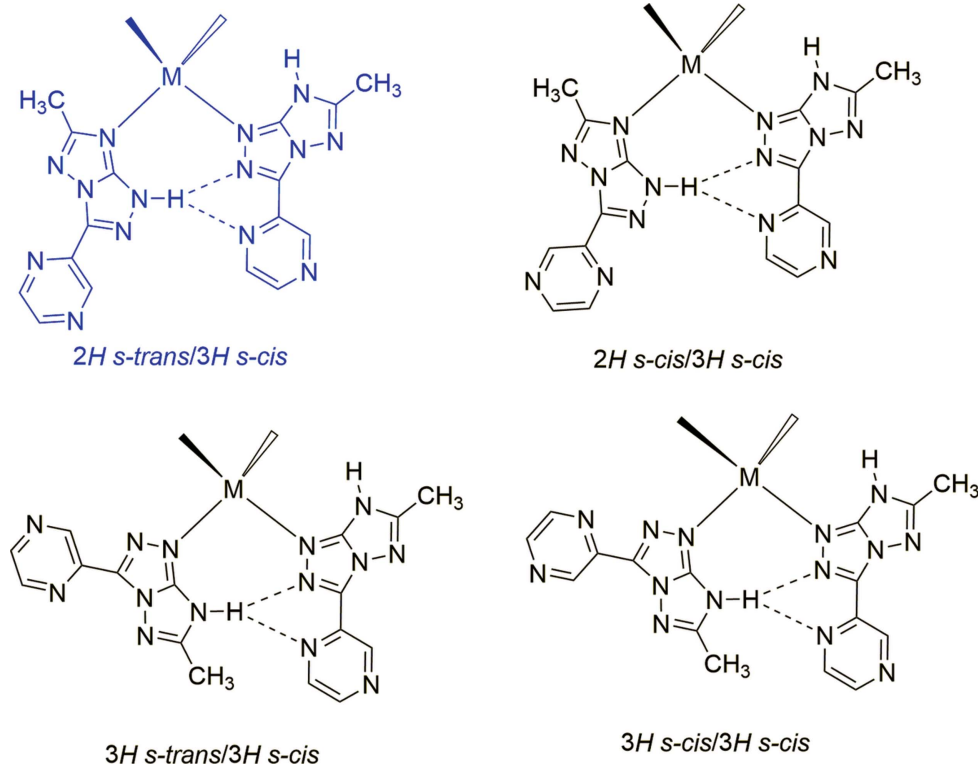


Figure 6

Hydrogen-bonded dimers of neutral TT9. The presence of a metal atom *M* in a tetrahedral coordination is also outlined. Highlighted in blue is the dimer found in complex **2**.

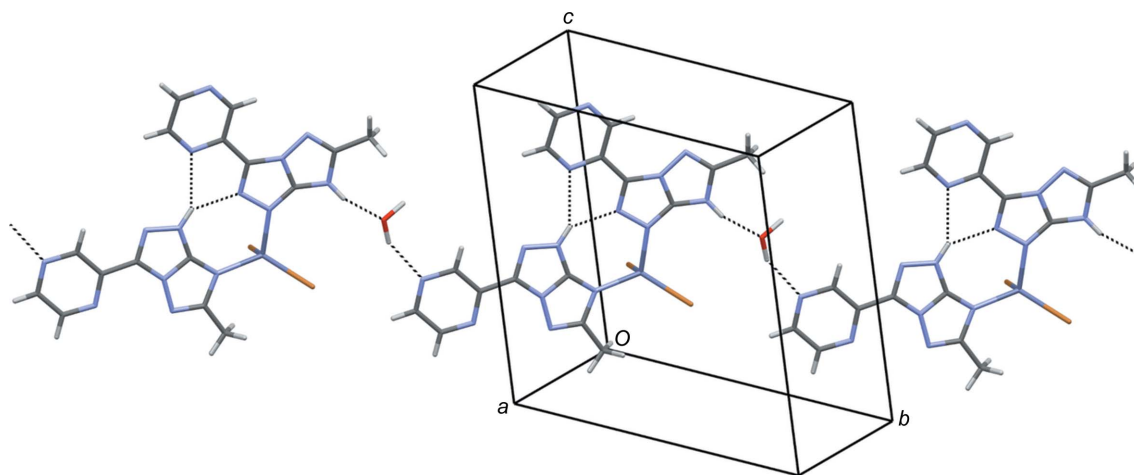


Figure 8
Partial crystal packing of complex **2**. Selected hydrogen bonds are indicated by dashed lines.

mer. While crystallization of pure TT9 from different solvents only affords the most stable *2H*-tautomer, we have proven that metal coordination allows selection of the elusive *3H*-tautomer. Depending on the stoichiometry of the complex, and on the metal, complexes with only the *3H*-tautomeric ligand (homotautomeric), or complexes with mixed-tautomer ligands, *i.e.* both *2H* and *3H* (heterotautomeric), can be obtained.

Steering and selectively controlling the formation of the different energetically feasible tautomers of a given compound, depending on the physico-chemical environment, is of practical and theoretical relevance. In fact, different tautomers generally interact differently with the same substrate and show different properties: in an analogy with language, they have different ‘meaning’. After all, chemistry can be considered a language: atoms are its letters and molecules its words. Continuing with this analogy, tautomers, and more generally isomers, would correspond to the anagrams of ordinary language. In this analogy, the heterotautomeric complex **2** would correspond to a sentence containing two anagrams of the same word, *e.g.* ‘she married an admirer’.

This is uncommon also in ordinary language.

Acknowledgements

The authors would like to acknowledge the contribution of the COST Action CA17120-Chemobrionics. Thanks are also due to the Centro Regionale di Competenza NTAP of Regione Campania (Italy) for the X-ray facility.

References

- Altomare, A., Burla, M. C., Camalli, M., Cascarano, G. L., Giacovazzo, C., Guagliardi, A., Moliterni, A. G. G., Polidori, G. & Spagna, R. (1999). *J. Appl. Cryst.* **32**, 115–119.
- Ambrosiano, P., Centore, R., Concilio, S., Panunzi, B., Sirigu, A. & Tirelli, N. (1999). *Polymer*, **40**, 4923–4928.
- Borbone, F., Caruso, U., Centore, R., DeMaria, A., Fort, A., Fusco, M., Panunzi, B., Roviello, A. & Tuzi, A. (2004). *Eur. J. Inorg. Chem.* **2004**, 2467–2476.
- Bruker (2001). *SADABS*. Bruker AXS Inc., Madison, Wisconsin, USA.
- Bussetti, G., Campione, M., Riva, M., Picone, A., Raimondo, L., Ferraro, L., Hogan, C., Palummo, M., Brambilla, A., Finazzi, M., Duò, L., Sassella, A. & Ciccacci, F. (2014). *Adv. Funct. Mater.* **24**, 958–963.
- Centore, R., Concilio, S., Panunzi, B., Sirigu, A. & Tirelli, N. (1999). *J. Polym. Sci. A Polym. Chem.* **37**, 603–608.
- Centore, R., Fusco, S., Capobianco, A., Piccialli, V., Zaccaria, S. & Peluso, A. (2013). *Eur. J. Org. Chem.* **2013**, 3721–3728.
- Centore, R., Manfredi, C., Capobianco, A., Volino, S., Ferrara, M. V., Carella, A., Fusco, S. & Peluso, A. (2017). *J. Org. Chem.* **82**, 5155–5161.
- Centore, R., Manfredi, C., Fusco, S., Maglione, C., Carella, A., Capobianco, A., Peluso, A., Colonna, D. & Di Carlo, A. (2015). *J. Mol. Struct.* **1093**, 119–124.
- Centore, R., Panunzi, B., Roviello, A., Sirigu, A. & Villano, P. (1996). *J. Polym. Sci. A Polym. Chem.* **34**, 3203–3211.
- Cotton, F. A., Wilkinson, G., Murillo, C. A. & Bochmann, M. (1999). In *Advanced Inorganic Chemistry*, 6th ed. New York: John Wiley & Sons Inc.
- Deneva, V., Dobrikov, G., Crochet, A., Nedeltcheva, D., Fromm, K. M. & Antonov, L. (2019). *J. Org. Chem.* **15**, 1898–1906.
- Duisenberg, A. J. M., Hooft, R. W. W., Schreurs, A. M. M. & Kroon, J. (2000). *J. Appl. Cryst.* **33**, 893–898.
- Duisenberg, A. J. M., Kroon-Batenburg, L. M. J. & Schreurs, A. M. M. (2003). *J. Appl. Cryst.* **36**, 220–229.
- Farrugia, L. J. (2012). *J. Appl. Cryst.* **45**, 849–854.
- Fusco, S., Parisi, E., Carella, A., Capobianco, A., Peluso, A., Manfredi, C., Borbone, F. & Centore, R. (2018). *Cryst. Growth Des.* **18**, 6293–6301.
- Goodman, M. (1995). *Nature*, **378**, 237–238.
- Horiuchi, S., Kobayashi, K., Kumai, R. & Ishibashi, S. (2017). *Nat. Commun.* **8**, 14426.
- Macrae, C. F., Sovago, I., Cottrell, S. J., Galek, P. T. A., McCabe, P., Pidcock, E., Platings, M., Shields, G. P., Stevens, J. S., Towler, M. & Wood, P. A. (2020). *J. Appl. Cryst.* **53**, 226–235.
- Martin, C. Y. (2009). *J. Comput. Aided Mol. Des.* **23**, 693–704.
- McNaught, A. D. & Wilkinson, A. (1997). In *IUPAC Compendium of Chemical Terminology*, 2nd ed. Oxford: Blackwell Science.
- Nonius (1999). *COLLECT*. Nonius BV, Delft, The Netherlands.
- Parisi, E., Capasso, D., Capobianco, A., Peluso, A., Di Gaetano, S., Fusco, S., Manfredi, C., Mozzillo, R., Pinto, G. & Centore, R. (2020). *Dalton Trans.* **49**, 14452–14462.
- Sheldrick, G. M. (2015). *Acta Cryst.* **C71**, 3–8.

- Sutradhar, M., Alegria, E. C. B. A., Mahmudov, T., Guedes da Silva, F. C. & Pompeiro, A. J. L. (2016). *RSC Adv.*, **6**, 8079–8088.
- Takjoo, R. & Centore, R. (2013). *J. Mol. Struct.* **1031**, 180–185.
- Taylor, P. J., Van der Zwan, G. & Antonov, L. (2014). In *Tautomerism: Methods and Theories*. Weinheim: Wiley-VCH Verlag GmbH & Co.
- Todorov, A. R., Nieger, M. & Helaja, J. (2012). *Chem. Eur. J.* **18**, 7269–7277.
- Wang, W., Hellinga, W. & Beese, L. S. (2011). *Proc. Natl Acad. Sci. USA*, **108**, 17644–17648.
- Watson, J. D. & Crick, F. H. (1953*a*). *Nature*, **171**, 737–738.
- Watson, J. D. & Crick, F. H. (1953*b*). *Nature*, **171**, 964–967.

supporting information

Acta Cryst. (2021). C77, 395-401 [https://doi.org/10.1107/S2053229621006203]

Stabilization of an elusive tautomer by metal coordination

Emmanuele Parisi and Roberto Centore

Computing details

For both structures, data collection: *COLLECT* (Nonius, 1999); cell refinement: *DIRAX/LSQ* (Duisenberg *et al.*, 2000); data reduction: *EVALCCD* (Duisenberg *et al.*, 2003); program(s) used to solve structure: *SIR97* (Altomare *et al.*, 1999); program(s) used to refine structure: *SHELXL2016* (Sheldrick, 2015); molecular graphics: *ORTEP-3 for Windows* (Farrugia, 2012) and *Mercury* (Macrae *et al.*, 2020); software used to prepare material for publication: *WinGX* (Farrugia, 2012).

Aquabromidobis[4-methyl-7-(pyrazin-2-yl)-3H-[1,2,4]triazolo[3,2-c][1,2,4]triazole]copper(II) bromide trihydrate (1)

Crystal data

[CuBr(C₈H₇N₇)₂(H₂O)]Br·3H₂O

$M_r = 697.83$

Monoclinic, *Cc*

$a = 11.062$ (4) Å

$b = 8.369$ (3) Å

$c = 27.406$ (6) Å

$\beta = 92.44$ (3)°

$V = 2534.9$ (14) Å³

$Z = 4$

$F(000) = 1388$

$D_x = 1.829$ Mg m⁻³

Mo $K\alpha$ radiation, $\lambda = 0.71073$ Å

Cell parameters from 320 reflections

$\theta = 3.3\text{--}28.5^\circ$

$\mu = 4.07$ mm⁻¹

$T = 173$ K

Prismatic, green

0.50 × 0.20 × 0.20 mm

Data collection

Bruker–Nonius KappaCCD
diffractometer

Radiation source: normal-focus sealed tube

Graphite monochromator

Detector resolution: 9 pixels mm⁻¹

CCD rotation images, thick slices scans

Absorption correction: multi-scan
(*SADABS*; Bruker, 2001)

$T_{\min} = 0.250$, $T_{\max} = 0.478$

8682 measured reflections

4870 independent reflections

4563 reflections with $I > 2\sigma(I)$

$R_{\text{int}} = 0.036$

$\theta_{\max} = 27.6^\circ$, $\theta_{\min} = 3.1^\circ$

$h = -13 \rightarrow 14$

$k = -10 \rightarrow 10$

$l = -35 \rightarrow 35$

Refinement

Refinement on F^2

Least-squares matrix: full

$R[F^2 > 2\sigma(F^2)] = 0.033$

$wR(F^2) = 0.081$

$S = 1.04$

4870 reflections

367 parameters

13 restraints

Primary atom site location: structure-invariant
direct methods

Secondary atom site location: difference Fourier
map

Hydrogen site location: mixed

H atoms treated by a mixture of independent
and constrained refinement

$$w = 1/[\sigma^2(F_o^2) + (0.0413P)^2 + 2.1083P]$$

$$\text{where } P = (F_o^2 + 2F_c^2)/3$$

$$(\Delta/\sigma)_{\max} < 0.001$$

$$\Delta\rho_{\max} = 0.60 \text{ e } \text{\AA}^{-3}$$

$$\Delta\rho_{\min} = -0.86 \text{ e } \text{\AA}^{-3}$$

Absolute structure: Refined as an inversion twin.

Absolute structure parameter: 0.502 (12)

Special details

Geometry. All esds (except the esd in the dihedral angle between two l.s. planes) are estimated using the full covariance matrix. The cell esds are taken into account individually in the estimation of esds in distances, angles and torsion angles; correlations between esds in cell parameters are only used when they are defined by crystal symmetry. An approximate (isotropic) treatment of cell esds is used for estimating esds involving l.s. planes.

Refinement. Refined as a 2-component inversion twin.

Data were collected on a Bruker-Nonius KappaCCD diffractometer equipped with Oxford Cryostream 700 apparatus. The structures were solved by direct methods and refined by the full matrix least squares method with anisotropic displacement parameters for non-H atoms.

Fractional atomic coordinates and isotropic or equivalent isotropic displacement parameters (\AA^2)

	x	y	z	$U_{\text{iso}}^*/U_{\text{eq}}$
C1A	0.2108 (5)	0.3482 (7)	0.1008 (2)	0.0171 (11)
C2A	0.0988 (5)	0.1833 (7)	0.0494 (2)	0.0203 (12)
H2A	0.055550	0.163375	0.019347	0.024*
C3A	0.1070 (6)	0.0641 (7)	0.0854 (2)	0.0233 (12)
H3A	0.070052	-0.036484	0.078759	0.028*
C4A	0.2180 (6)	0.2281 (7)	0.1359 (2)	0.0218 (12)
H4A	0.261924	0.247106	0.165862	0.026*
C5A	0.2645 (5)	0.5042 (7)	0.1058 (2)	0.0164 (11)
C6A	0.3529 (5)	0.7240 (7)	0.1263 (2)	0.0177 (11)
C7A	0.4323 (6)	0.6809 (8)	0.1994 (2)	0.0227 (12)
C8A	0.5012 (7)	0.7127 (9)	0.2462 (2)	0.0322 (15)
H8A	0.448925	0.767907	0.268770	0.048*
H8B	0.571526	0.779821	0.240018	0.048*
H8C	0.528625	0.611249	0.260743	0.048*
N1A	0.2503 (5)	0.6096 (6)	0.07033 (17)	0.0184 (10)
N2A	0.3066 (5)	0.7527 (6)	0.08205 (18)	0.0195 (10)
N3A	0.4212 (5)	0.7944 (6)	0.16306 (18)	0.0195 (10)
H3NA	0.461 (6)	0.882 (5)	0.162 (3)	0.023*
N4A	0.3787 (5)	0.5451 (6)	0.18878 (17)	0.0219 (10)
N5A	0.3309 (4)	0.5749 (6)	0.14234 (16)	0.0160 (9)
N6A	0.1518 (4)	0.3249 (5)	0.05743 (18)	0.0180 (10)
N7A	0.1644 (5)	0.0863 (6)	0.12843 (18)	0.0226 (11)
C1B	0.1316 (5)	0.6931 (7)	-0.0809 (2)	0.0184 (11)
C2B	0.1366 (6)	0.7999 (7)	-0.1188 (2)	0.0212 (12)
H2B	0.101996	0.771551	-0.149940	0.025*
C3B	0.2360 (6)	0.9747 (8)	-0.0686 (2)	0.0252 (13)
H3B	0.272402	1.076143	-0.062860	0.030*
C4B	0.2340 (6)	0.8649 (7)	-0.0299 (2)	0.0214 (12)
H4B	0.270875	0.891593	0.000938	0.026*
C5B	0.0785 (6)	0.5357 (7)	-0.0844 (2)	0.0190 (12)
C6B	-0.0024 (5)	0.3091 (7)	-0.1041 (2)	0.0191 (11)

C7B	-0.0630 (6)	0.3334 (7)	-0.1805 (2)	0.0236 (12)
C8B	-0.1181 (7)	0.2884 (9)	-0.2287 (2)	0.0335 (16)
H8D	-0.123800	0.382944	-0.249744	0.050*
H8E	-0.199277	0.244961	-0.224433	0.050*
H8F	-0.067814	0.207352	-0.243794	0.050*
N1B	0.0837 (4)	0.4380 (6)	-0.04658 (18)	0.0191 (10)
N2B	0.0320 (5)	0.2912 (6)	-0.05801 (18)	0.0209 (10)
N3B	-0.0583 (5)	0.2296 (6)	-0.14155 (18)	0.0214 (10)
H3NB	-0.088 (6)	0.137 (5)	-0.137 (3)	0.026*
N4B	-0.0137 (5)	0.4731 (6)	-0.17061 (17)	0.0206 (11)
N5B	0.0225 (4)	0.4554 (6)	-0.12167 (17)	0.0182 (10)
N6B	0.1811 (4)	0.7247 (6)	-0.03631 (17)	0.0160 (9)
N7B	0.1890 (5)	0.9421 (6)	-0.1129 (2)	0.0267 (12)
O1	0.3589 (5)	0.4611 (5)	-0.01555 (18)	0.0310 (10)
H1W	0.381 (8)	0.372 (5)	-0.005 (2)	0.037*
H2W	0.362 (7)	0.449 (8)	-0.0455 (10)	0.037*
O2	0.5055 (6)	1.0913 (6)	0.15962 (18)	0.0420 (13)
H3W	0.492 (9)	1.114 (11)	0.1310 (13)	0.050*
H4W	0.543 (8)	1.161 (8)	0.174 (3)	0.050*
O3	0.1544 (5)	-0.1814 (5)	0.19710 (16)	0.0298 (11)
H5W	0.136 (8)	-0.139 (8)	0.2215 (19)	0.036*
H6W	0.176 (8)	-0.108 (7)	0.181 (3)	0.036*
O4	0.1829 (6)	1.1261 (6)	-0.20431 (19)	0.0400 (13)
H7W	0.177 (9)	1.080 (10)	-0.1778 (18)	0.048*
H8W	0.229 (6)	1.200 (7)	-0.199 (3)	0.048*
Br1	-0.05312 (4)	0.64638 (7)	0.04411 (2)	0.02344 (15)
Br2	-0.16760 (5)	-0.12171 (7)	-0.13330 (2)	0.03047 (17)
Cu	0.16163 (6)	0.52924 (8)	0.01225 (3)	0.01672 (15)

Atomic displacement parameters (Å²)

	U^{11}	U^{22}	U^{33}	U^{12}	U^{13}	U^{23}
C1A	0.019 (3)	0.016 (3)	0.016 (2)	0.003 (2)	-0.001 (2)	0.001 (2)
C2A	0.020 (3)	0.016 (3)	0.025 (3)	0.001 (2)	0.000 (2)	-0.001 (2)
C3A	0.027 (3)	0.018 (3)	0.026 (3)	-0.003 (2)	0.004 (2)	-0.001 (2)
C4A	0.023 (3)	0.023 (3)	0.019 (3)	0.001 (2)	0.001 (2)	0.005 (2)
C5A	0.016 (3)	0.018 (3)	0.014 (2)	0.001 (2)	-0.004 (2)	0.001 (2)
C6A	0.017 (3)	0.015 (3)	0.021 (3)	-0.001 (2)	0.001 (2)	0.000 (2)
C7A	0.022 (3)	0.028 (3)	0.018 (2)	0.003 (3)	-0.001 (2)	-0.001 (2)
C8A	0.039 (4)	0.034 (4)	0.022 (3)	-0.002 (3)	-0.011 (3)	-0.005 (3)
N1A	0.020 (3)	0.015 (2)	0.020 (2)	-0.0028 (19)	-0.001 (2)	-0.0004 (18)
N2A	0.023 (3)	0.014 (2)	0.021 (2)	-0.007 (2)	-0.005 (2)	-0.0019 (19)
N3A	0.021 (3)	0.019 (3)	0.018 (2)	0.000 (2)	-0.005 (2)	0.0017 (19)
N4A	0.026 (3)	0.024 (3)	0.015 (2)	0.001 (2)	-0.004 (2)	0.0015 (19)
N5A	0.018 (2)	0.013 (2)	0.016 (2)	-0.0007 (18)	-0.0020 (19)	0.0007 (17)
N6A	0.019 (2)	0.015 (2)	0.021 (2)	0.0009 (19)	0.0037 (19)	0.0017 (18)
N7A	0.028 (3)	0.015 (2)	0.025 (2)	0.001 (2)	0.001 (2)	0.0028 (19)
C1B	0.016 (3)	0.018 (3)	0.021 (2)	0.004 (2)	0.003 (2)	0.002 (2)

C2B	0.026 (3)	0.019 (3)	0.018 (3)	-0.002 (2)	-0.004 (2)	0.002 (2)
C3B	0.023 (3)	0.023 (3)	0.029 (3)	0.001 (2)	-0.004 (3)	0.002 (3)
C4B	0.021 (3)	0.023 (3)	0.020 (3)	0.001 (2)	-0.003 (2)	0.000 (2)
C5B	0.023 (3)	0.017 (3)	0.017 (2)	-0.001 (2)	0.003 (2)	0.003 (2)
C6B	0.020 (3)	0.016 (3)	0.022 (3)	-0.001 (2)	0.002 (2)	0.001 (2)
C7B	0.025 (3)	0.025 (3)	0.020 (3)	0.003 (3)	-0.002 (2)	-0.001 (2)
C8B	0.043 (4)	0.033 (4)	0.024 (3)	-0.004 (3)	-0.005 (3)	-0.007 (3)
N1B	0.021 (3)	0.018 (2)	0.018 (2)	-0.0035 (19)	-0.0010 (19)	0.0033 (19)
N2B	0.025 (3)	0.017 (2)	0.020 (2)	-0.005 (2)	-0.005 (2)	-0.0017 (19)
N3B	0.024 (3)	0.018 (3)	0.022 (2)	-0.003 (2)	-0.007 (2)	-0.0026 (19)
N4B	0.026 (3)	0.022 (3)	0.014 (2)	0.000 (2)	-0.004 (2)	-0.0011 (19)
N5B	0.019 (2)	0.019 (3)	0.016 (2)	-0.0033 (19)	-0.0054 (19)	0.0015 (18)
N6B	0.016 (2)	0.015 (2)	0.017 (2)	0.0018 (18)	-0.0029 (19)	0.0031 (17)
N7B	0.028 (3)	0.022 (3)	0.030 (3)	0.000 (2)	-0.001 (2)	0.006 (2)
O1	0.038 (3)	0.024 (2)	0.031 (2)	0.008 (2)	0.003 (2)	0.0046 (19)
O2	0.068 (4)	0.032 (3)	0.026 (2)	-0.023 (3)	-0.006 (3)	0.002 (2)
O3	0.041 (3)	0.022 (2)	0.027 (3)	-0.006 (2)	0.002 (2)	0.0006 (18)
O4	0.057 (4)	0.035 (3)	0.026 (2)	-0.013 (3)	-0.009 (3)	0.005 (2)
Br1	0.0212 (3)	0.0251 (3)	0.0239 (3)	0.0039 (2)	0.0000 (2)	0.0014 (2)
Br2	0.0303 (4)	0.0254 (3)	0.0363 (3)	-0.0067 (3)	0.0068 (3)	-0.0072 (3)
Cu	0.0210 (3)	0.0142 (3)	0.0144 (3)	-0.0030 (3)	-0.0043 (2)	0.0018 (3)

Geometric parameters (Å, °)

C1A—N6A	1.346 (8)	C3B—N7B	1.329 (9)
C1A—C4A	1.391 (8)	C3B—C4B	1.403 (9)
C1A—C5A	1.438 (8)	C3B—H3B	0.9500
C2A—N6A	1.336 (7)	C4B—N6B	1.320 (8)
C2A—C3A	1.404 (9)	C4B—H4B	0.9500
C2A—H2A	0.9500	C5B—N1B	1.320 (7)
C3A—N7A	1.328 (8)	C5B—N5B	1.350 (8)
C3A—H3A	0.9500	C6B—N2B	1.311 (8)
C4A—N7A	1.338 (8)	C6B—N5B	1.349 (7)
C4A—H4A	0.9500	C6B—N3B	1.352 (8)
C5A—N1A	1.317 (7)	C7B—N4B	1.313 (8)
C5A—N5A	1.353 (7)	C7B—N3B	1.376 (8)
C6A—N2A	1.317 (8)	C7B—C8B	1.480 (9)
C6A—N5A	1.349 (7)	C8B—H8D	0.9800
C6A—N3A	1.368 (8)	C8B—H8E	0.9800
C7A—N4A	1.310 (8)	C8B—H8F	0.9800
C7A—N3A	1.378 (8)	N1B—N2B	1.385 (7)
C7A—C8A	1.489 (8)	N1B—Cu	1.951 (5)
C8A—H8A	0.9800	N3B—H3NB	0.85 (3)
C8A—H8B	0.9800	N4B—N5B	1.391 (6)
C8A—H8C	0.9800	N6B—Cu	2.125 (5)
N1A—N2A	1.382 (7)	O1—Cu	2.410 (5)
N1A—Cu	1.953 (5)	O1—H1W	0.83 (3)
N3A—H3NA	0.86 (3)	O1—H2W	0.83 (3)

N4A—N5A	1.380 (7)	O2—H3W	0.82 (3)
N6A—Cu	2.117 (5)	O2—H4W	0.81 (3)
C1B—N6B	1.343 (7)	O3—H5W	0.79 (3)
C1B—C2B	1.374 (8)	O3—H6W	0.80 (3)
C1B—C5B	1.444 (8)	O4—H7W	0.83 (3)
C2B—N7B	1.331 (8)	O4—H8W	0.81 (3)
C2B—H2B	0.9500	Br1—Cu	2.7466 (12)
N6A—C1A—C4A	121.1 (5)	C3B—C4B—H4B	119.9
N6A—C1A—C5A	113.4 (5)	N1B—C5B—N5B	106.8 (5)
C4A—C1A—C5A	125.5 (5)	N1B—C5B—C1B	120.5 (6)
N6A—C2A—C3A	120.0 (6)	N5B—C5B—C1B	132.6 (5)
N6A—C2A—H2A	120.0	N2B—C6B—N5B	113.1 (5)
C3A—C2A—H2A	120.0	N2B—C6B—N3B	141.3 (5)
N7A—C3A—C2A	122.6 (6)	N5B—C6B—N3B	105.6 (5)
N7A—C3A—H3A	118.7	N4B—C7B—N3B	113.6 (5)
C2A—C3A—H3A	118.7	N4B—C7B—C8B	124.2 (6)
N7A—C4A—C1A	121.6 (6)	N3B—C7B—C8B	122.1 (6)
N7A—C4A—H4A	119.2	C7B—C8B—H8D	109.5
C1A—C4A—H4A	119.2	C7B—C8B—H8E	109.5
N1A—C5A—N5A	107.3 (5)	H8D—C8B—H8E	109.5
N1A—C5A—C1A	120.2 (5)	C7B—C8B—H8F	109.5
N5A—C5A—C1A	132.5 (5)	H8D—C8B—H8F	109.5
N2A—C6A—N5A	113.6 (5)	H8E—C8B—H8F	109.5
N2A—C6A—N3A	141.3 (5)	C5B—N1B—N2B	111.6 (5)
N5A—C6A—N3A	105.0 (5)	C5B—N1B—Cu	114.2 (4)
N4A—C7A—N3A	114.4 (5)	N2B—N1B—Cu	134.2 (4)
N4A—C7A—C8A	123.9 (6)	C6B—N2B—N1B	102.5 (5)
N3A—C7A—C8A	121.8 (6)	C6B—N3B—C7B	106.2 (5)
C7A—C8A—H8A	109.5	C6B—N3B—H3NB	119 (5)
C7A—C8A—H8B	109.5	C7B—N3B—H3NB	134 (5)
H8A—C8A—H8B	109.5	C7B—N4B—N5B	101.8 (5)
C7A—C8A—H8C	109.5	C6B—N5B—C5B	106.0 (5)
H8A—C8A—H8C	109.5	C6B—N5B—N4B	112.7 (5)
H8B—C8A—H8C	109.5	C5B—N5B—N4B	141.2 (5)
C5A—N1A—N2A	111.8 (5)	C4B—N6B—C1B	117.2 (5)
C5A—N1A—Cu	114.2 (4)	C4B—N6B—Cu	131.1 (4)
N2A—N1A—Cu	133.9 (4)	C1B—N6B—Cu	111.7 (4)
C6A—N2A—N1A	102.1 (5)	C3B—N7B—C2B	116.5 (5)
C6A—N3A—C7A	105.4 (5)	Cu—O1—H1W	111 (6)
C6A—N3A—H3NA	128 (5)	Cu—O1—H2W	115 (6)
C7A—N3A—H3NA	126 (5)	H1W—O1—H2W	101 (4)
C7A—N4A—N5A	101.5 (5)	H3W—O2—H4W	112 (9)
C6A—N5A—C5A	105.2 (5)	H5W—O3—H6W	103 (8)
C6A—N5A—N4A	113.7 (5)	H7W—O4—H8W	105 (9)
C5A—N5A—N4A	141.1 (5)	N1B—Cu—N1A	175.5 (2)
C2A—N6A—C1A	117.8 (5)	N1B—Cu—N6A	97.78 (19)
C2A—N6A—Cu	130.8 (4)	N1A—Cu—N6A	80.67 (19)

C1A—N6A—Cu	111.4 (4)	N1B—Cu—N6B	80.60 (19)
C3A—N7A—C4A	116.8 (5)	N1A—Cu—N6B	100.64 (19)
N6B—C1B—C2B	122.2 (5)	N6A—Cu—N6B	175.62 (18)
N6B—C1B—C5B	113.0 (5)	N1B—Cu—O1	91.16 (19)
C2B—C1B—C5B	124.8 (5)	N1A—Cu—O1	84.78 (19)
N7B—C2B—C1B	121.4 (6)	N6A—Cu—O1	93.64 (17)
N7B—C2B—H2B	119.3	N6B—Cu—O1	82.35 (17)
C1B—C2B—H2B	119.3	N1B—Cu—Br1	92.56 (15)
N7B—C3B—C4B	122.5 (6)	N1A—Cu—Br1	91.68 (15)
N7B—C3B—H3B	118.7	N6A—Cu—Br1	92.06 (13)
C4B—C3B—H3B	118.7	N6B—Cu—Br1	92.08 (13)
N6B—C4B—C3B	120.2 (6)	O1—Cu—Br1	172.72 (11)
N6B—C4B—H4B	119.9		
N6A—C2A—C3A—N7A	1.2 (9)	N6B—C1B—C2B—N7B	-1.4 (9)
N6A—C1A—C4A—N7A	-1.6 (9)	C5B—C1B—C2B—N7B	-178.9 (5)
C5A—C1A—C4A—N7A	179.5 (5)	N7B—C3B—C4B—N6B	-1.9 (10)
N6A—C1A—C5A—N1A	2.0 (8)	N6B—C1B—C5B—N1B	-1.3 (8)
C4A—C1A—C5A—N1A	-179.0 (6)	C2B—C1B—C5B—N1B	176.3 (6)
N6A—C1A—C5A—N5A	-179.4 (6)	N6B—C1B—C5B—N5B	-178.6 (6)
C4A—C1A—C5A—N5A	-0.5 (10)	C2B—C1B—C5B—N5B	-1.0 (10)
N5A—C5A—N1A—N2A	0.1 (6)	N5B—C5B—N1B—N2B	0.3 (6)
C1A—C5A—N1A—N2A	179.0 (5)	C1B—C5B—N1B—N2B	-177.6 (5)
N5A—C5A—N1A—Cu	177.7 (3)	N5B—C5B—N1B—Cu	-179.9 (4)
C1A—C5A—N1A—Cu	-3.4 (7)	C1B—C5B—N1B—Cu	2.2 (7)
N5A—C6A—N2A—N1A	0.8 (6)	N5B—C6B—N2B—N1B	-0.8 (6)
N3A—C6A—N2A—N1A	178.5 (7)	N3B—C6B—N2B—N1B	-179.3 (8)
C5A—N1A—N2A—C6A	-0.5 (6)	C5B—N1B—N2B—C6B	0.3 (6)
Cu—N1A—N2A—C6A	-177.5 (4)	Cu—N1B—N2B—C6B	-179.4 (4)
N2A—C6A—N3A—C7A	-179.3 (8)	N2B—C6B—N3B—C7B	179.2 (8)
N5A—C6A—N3A—C7A	-1.4 (6)	N5B—C6B—N3B—C7B	0.6 (6)
N4A—C7A—N3A—C6A	0.7 (7)	N4B—C7B—N3B—C6B	0.3 (7)
C8A—C7A—N3A—C6A	-179.9 (6)	C8B—C7B—N3B—C6B	179.9 (6)
N3A—C7A—N4A—N5A	0.3 (7)	N3B—C7B—N4B—N5B	-1.0 (6)
C8A—C7A—N4A—N5A	-179.1 (6)	C8B—C7B—N4B—N5B	179.4 (6)
N2A—C6A—N5A—C5A	-0.7 (7)	N2B—C6B—N5B—C5B	1.0 (7)
N3A—C6A—N5A—C5A	-179.3 (4)	N3B—C6B—N5B—C5B	-179.9 (5)
N2A—C6A—N5A—N4A	-179.6 (5)	N2B—C6B—N5B—N4B	179.6 (5)
N3A—C6A—N5A—N4A	1.8 (6)	N3B—C6B—N5B—N4B	-1.3 (6)
N1A—C5A—N5A—C6A	0.3 (6)	N1B—C5B—N5B—C6B	-0.8 (6)
C1A—C5A—N5A—C6A	-178.4 (6)	C1B—C5B—N5B—C6B	176.8 (6)
N1A—C5A—N5A—N4A	178.8 (6)	N1B—C5B—N5B—N4B	-178.7 (6)
C1A—C5A—N5A—N4A	0.1 (12)	C1B—C5B—N5B—N4B	-1.2 (12)
C7A—N4A—N5A—C6A	-1.3 (6)	C7B—N4B—N5B—C6B	1.4 (6)
C7A—N4A—N5A—C5A	-179.7 (7)	C7B—N4B—N5B—C5B	179.3 (7)
C3A—C2A—N6A—C1A	-0.8 (8)	C3B—C4B—N6B—C1B	0.6 (8)
C3A—C2A—N6A—Cu	178.8 (4)	C3B—C4B—N6B—Cu	179.2 (4)
C4A—C1A—N6A—C2A	1.0 (8)	C2B—C1B—N6B—C4B	1.0 (8)

C5A—C1A—N6A—C2A	−180.0 (5)	C5B—C1B—N6B—C4B	178.7 (5)
C4A—C1A—N6A—Cu	−178.7 (4)	C2B—C1B—N6B—Cu	−177.8 (5)
C5A—C1A—N6A—Cu	0.3 (6)	C5B—C1B—N6B—Cu	−0.1 (6)
C2A—C3A—N7A—C4A	−1.7 (8)	C4B—C3B—N7B—C2B	1.5 (9)
C1A—C4A—N7A—C3A	1.9 (8)	C1B—C2B—N7B—C3B	0.2 (9)

Hydrogen-bond geometry (Å, °)

<i>D</i> —H... <i>A</i>	<i>D</i> —H	H... <i>A</i>	<i>D</i> ... <i>A</i>	<i>D</i> —H... <i>A</i>
C2A—H2A...N2B	0.95	2.38	3.137 (8)	137
C3A—H3A...Br1 ⁱ	0.95	3.11	4.058 (6)	173
N3A—H3NA...O2	0.86 (3)	1.82 (3)	2.657 (7)	165 (7)
C4B—H4B...N2A	0.95	2.52	3.276 (8)	136
C4B—H4B...Br1 ⁱⁱ	0.95	3.09	3.848 (6)	138
N3B—H3NB...Br2	0.85 (3)	2.34 (3)	3.190 (5)	173 (7)
O1—H1W...Br1 ⁱⁱⁱ	0.83 (3)	2.42 (3)	3.229 (5)	166 (6)
O1—H2W...Br2 ⁱⁱ	0.83 (3)	2.49 (3)	3.301 (5)	168 (8)
O2—H3W...Br1 ⁱⁱ	0.82 (3)	2.43 (3)	3.237 (5)	173 (9)
O2—H4W...O3 ^{iv}	0.81 (3)	1.89 (4)	2.691 (7)	167 (10)
O3—H5W...O4 ^v	0.79 (3)	2.08 (6)	2.746 (7)	141 (8)
O3—H6W...N7A	0.80 (3)	2.17 (4)	2.931 (7)	159 (9)
O4—H7W...N7B	0.83 (3)	2.12 (3)	2.939 (7)	171 (9)
O4—H8W...Br2 ^{iv}	0.81 (3)	2.56 (6)	3.272 (6)	147 (8)

Symmetry codes: (i) *x*, *y*−1, *z*; (ii) *x*+1/2, *y*+1/2, *z*; (iii) *x*+1/2, *y*−1/2, *z*; (iv) *x*+1/2, *y*+3/2, *z*; (v) *x*, −*y*+1, *z*+1/2.

Dibromido[4-methyl-7-(pyrazin-2-yl)-2*H*-[1,2,4]triazolo[3,2-*c*][1,2,4]triazole][4-methyl-7-(pyrazin-2-yl)-3*H*-[1,2,4]triazolo[3,2-*c*][1,2,4]triazole]zinc(II) monohydrate (2)

Crystal data

[ZnBr₂(C₈H₇N₇)₂]·H₂O

*M*_r = 645.62

Triclinic, *P*1

a = 8.396 (2) Å

b = 12.305 (3) Å

c = 12.724 (3) Å

α = 112.53 (2)°

β = 107.78 (3)°

γ = 92.16 (2)°

V = 1138.1 (5) Å³

Z = 2

F(000) = 636

*D*_x = 1.884 Mg m^{−3}

Mo *K*α radiation, λ = 0.71073 Å

Cell parameters from 467 reflections

θ = 2.5–29.4°

μ = 4.63 mm^{−1}

T = 293 K

Prismatic, brown

0.40 × 0.30 × 0.20 mm

Data collection

Bruker–Nonius KappaCCD
diffractometer

Radiation source: normal-focus sealed tube

Graphite monochromator

Detector resolution: 9 pixels mm^{−1}

CCD rotation images, thick slices scans

Absorption correction: multi-scan

(*SADABS*; Bruker, 2001)

*T*_{min} = 0.270, *T*_{max} = 0.433

12306 measured reflections

5090 independent reflections

3636 reflections with *I* > 2σ(*I*)

*R*_{int} = 0.042

θ_{max} = 27.5°, θ_{min} = 3.0°

h = −10→9

k = −15→15

l = −16→16

Refinement

Refinement on F^2

Least-squares matrix: full

$R[F^2 > 2\sigma(F^2)] = 0.047$

$wR(F^2) = 0.136$

$S = 1.09$

5090 reflections

315 parameters

2 restraints

Primary atom site location: structure-invariant
direct methods

Secondary atom site location: difference Fourier
map

Hydrogen site location: mixed

H atoms treated by a mixture of independent
and constrained refinement

$w = 1/[\sigma^2(F_o^2) + (0.0621P)^2 + 1.6216P]$

where $P = (F_o^2 + 2F_c^2)/3$

$(\Delta/\sigma)_{\max} < 0.001$

$\Delta\rho_{\max} = 0.70 \text{ e } \text{\AA}^{-3}$

$\Delta\rho_{\min} = -0.74 \text{ e } \text{\AA}^{-3}$

Special details

Geometry. All esds (except the esd in the dihedral angle between two l.s. planes) are estimated using the full covariance matrix. The cell esds are taken into account individually in the estimation of esds in distances, angles and torsion angles; correlations between esds in cell parameters are only used when they are defined by crystal symmetry. An approximate (isotropic) treatment of cell esds is used for estimating esds involving l.s. planes.

Refinement. Data were collected on a Bruker-Nonius KappaCCD diffractometer equipped with Oxford Cryostream 700 apparatus. The structures were solved by direct methods and refined by the full matrix least squares method with anisotropic displacement parameters for non-H atoms.

Fractional atomic coordinates and isotropic or equivalent isotropic displacement parameters (\AA^2)

	<i>x</i>	<i>y</i>	<i>z</i>	$U_{\text{iso}}^*/U_{\text{eq}}$
C1A	0.7622 (6)	-0.1592 (4)	0.2765 (5)	0.0327 (10)
C2A	0.8753 (7)	-0.1982 (5)	0.3538 (5)	0.0419 (12)
H2A	0.910796	-0.152912	0.437155	0.050*
C3A	0.8825 (7)	-0.3578 (5)	0.1909 (6)	0.0473 (13)
H3A	0.919272	-0.429248	0.157203	0.057*
C4A	0.7757 (8)	-0.3151 (5)	0.1150 (6)	0.0499 (14)
H4A	0.747553	-0.357230	0.031646	0.060*
C5A	0.6867 (6)	-0.0542 (4)	0.3258 (5)	0.0328 (10)
C6A	0.5263 (6)	0.0829 (4)	0.3413 (4)	0.0323 (10)
C7A	0.3906 (6)	0.0624 (5)	0.1628 (5)	0.0394 (11)
C8A	0.2693 (8)	0.0807 (7)	0.0606 (5)	0.0581 (17)
H8A	0.273891	0.023930	-0.014849	0.087*
H8B	0.299509	0.160286	0.068690	0.087*
H8C	0.156311	0.069745	0.061995	0.087*
N1A	0.7145 (5)	0.0033 (4)	0.4421 (4)	0.0394 (10)
N2A	0.6147 (6)	0.0897 (4)	0.4513 (4)	0.0391 (10)
H2NA	0.607 (7)	0.138 (4)	0.517 (3)	0.047*
N3A	0.4115 (5)	0.1312 (4)	0.2834 (4)	0.0352 (9)
N4A	0.4836 (5)	-0.0220 (4)	0.1438 (4)	0.0394 (10)
N5A	0.5711 (5)	-0.0065 (4)	0.2614 (4)	0.0334 (9)
N6A	0.7115 (6)	-0.2166 (4)	0.1556 (4)	0.0445 (11)
N7A	0.9342 (6)	-0.2990 (4)	0.3114 (5)	0.0472 (11)
C1B	0.6464 (6)	0.3015 (4)	0.7817 (4)	0.0335 (10)
C2B	0.7013 (8)	0.3681 (5)	0.9056 (5)	0.0525 (15)
H2B	0.653069	0.434809	0.935948	0.063*
C3B	0.8740 (8)	0.2402 (6)	0.9334 (6)	0.0560 (16)

H3B	0.954592	0.215786	0.984276	0.067*
C4B	0.8170 (7)	0.1699 (5)	0.8100 (6)	0.0476 (14)
H4B	0.860005	0.100278	0.780550	0.057*
C5B	0.5245 (6)	0.3357 (4)	0.6953 (4)	0.0333 (10)
C6B	0.3573 (6)	0.4326 (4)	0.6126 (5)	0.0364 (11)
C7B	0.3548 (6)	0.5944 (4)	0.7617 (5)	0.0352 (10)
C8B	0.3150 (7)	0.7132 (5)	0.8251 (6)	0.0474 (13)
H8D	0.201770	0.703714	0.826530	0.071*
H8E	0.323254	0.762347	0.783202	0.071*
H8F	0.394277	0.750544	0.906771	0.071*
N1B	0.4712 (6)	0.2739 (4)	0.5773 (4)	0.0408 (10)
N2B	0.3645 (5)	0.3337 (4)	0.5216 (4)	0.0412 (10)
N3B	0.2928 (5)	0.5339 (4)	0.6371 (4)	0.0376 (10)
H3NB	0.245 (6)	0.563 (5)	0.588 (4)	0.045*
N4B	0.4512 (5)	0.5378 (4)	0.8169 (4)	0.0351 (9)
N5B	0.4513 (5)	0.4356 (3)	0.7202 (3)	0.0310 (8)
N6B	0.7007 (5)	0.2004 (4)	0.7322 (4)	0.0388 (10)
N7B	0.8197 (7)	0.3407 (5)	0.9827 (5)	0.0585 (14)
Zn	0.25393 (7)	0.24715 (5)	0.33982 (5)	0.03379 (16)
Br1	0.00038 (7)	0.11388 (5)	0.29176 (6)	0.04583 (17)
Br2	0.20342 (8)	0.39584 (6)	0.26552 (7)	0.0577 (2)
O1W	0.1184 (9)	0.6539 (6)	0.5184 (5)	0.103 (2)
H1W	0.061280	0.710175	0.572921	0.124*
H2W	0.050768	0.636549	0.434186	0.124*

Atomic displacement parameters (Å²)

	U^{11}	U^{22}	U^{33}	U^{12}	U^{13}	U^{23}
C1A	0.034 (2)	0.031 (2)	0.036 (3)	0.0062 (18)	0.013 (2)	0.015 (2)
C2A	0.044 (3)	0.046 (3)	0.038 (3)	0.013 (2)	0.015 (2)	0.019 (3)
C3A	0.052 (3)	0.036 (3)	0.053 (4)	0.015 (2)	0.022 (3)	0.014 (3)
C4A	0.058 (3)	0.042 (3)	0.040 (3)	0.009 (3)	0.014 (3)	0.009 (3)
C5A	0.033 (2)	0.033 (2)	0.034 (3)	0.0084 (19)	0.012 (2)	0.016 (2)
C6A	0.030 (2)	0.035 (2)	0.029 (3)	0.0062 (18)	0.0089 (19)	0.010 (2)
C7A	0.034 (2)	0.051 (3)	0.033 (3)	0.010 (2)	0.011 (2)	0.018 (2)
C8A	0.056 (4)	0.081 (5)	0.034 (3)	0.032 (3)	0.012 (3)	0.022 (3)
N1A	0.046 (2)	0.039 (2)	0.037 (2)	0.0150 (18)	0.0148 (19)	0.018 (2)
N2A	0.046 (2)	0.041 (2)	0.028 (2)	0.0166 (19)	0.0121 (19)	0.0122 (19)
N3A	0.033 (2)	0.044 (2)	0.030 (2)	0.0121 (17)	0.0098 (17)	0.0169 (19)
N4A	0.041 (2)	0.046 (2)	0.030 (2)	0.0111 (18)	0.0093 (18)	0.015 (2)
N5A	0.033 (2)	0.035 (2)	0.031 (2)	0.0075 (16)	0.0090 (17)	0.0143 (18)
N6A	0.050 (3)	0.040 (2)	0.038 (3)	0.009 (2)	0.010 (2)	0.015 (2)
N7A	0.054 (3)	0.044 (3)	0.049 (3)	0.018 (2)	0.019 (2)	0.022 (2)
C1B	0.037 (2)	0.031 (2)	0.031 (3)	0.0064 (19)	0.007 (2)	0.013 (2)
C2B	0.064 (4)	0.045 (3)	0.034 (3)	0.020 (3)	0.001 (3)	0.013 (3)
C3B	0.057 (4)	0.064 (4)	0.053 (4)	0.018 (3)	0.008 (3)	0.038 (3)
C4B	0.046 (3)	0.041 (3)	0.060 (4)	0.017 (2)	0.016 (3)	0.027 (3)
C5B	0.036 (2)	0.029 (2)	0.030 (3)	0.0048 (18)	0.009 (2)	0.009 (2)

C6B	0.036 (2)	0.036 (3)	0.033 (3)	0.0078 (19)	0.006 (2)	0.014 (2)
C7B	0.032 (2)	0.038 (3)	0.038 (3)	0.0065 (19)	0.015 (2)	0.016 (2)
C8B	0.055 (3)	0.039 (3)	0.052 (4)	0.022 (2)	0.024 (3)	0.018 (3)
N1B	0.047 (2)	0.037 (2)	0.032 (2)	0.0122 (18)	0.0070 (19)	0.0116 (19)
N2B	0.043 (2)	0.039 (2)	0.034 (2)	0.0134 (18)	0.0041 (19)	0.013 (2)
N3B	0.037 (2)	0.040 (2)	0.036 (2)	0.0131 (18)	0.0079 (18)	0.019 (2)
N4B	0.040 (2)	0.032 (2)	0.029 (2)	0.0082 (17)	0.0104 (17)	0.0097 (18)
N5B	0.036 (2)	0.0290 (19)	0.023 (2)	0.0067 (16)	0.0060 (16)	0.0093 (16)
N6B	0.038 (2)	0.034 (2)	0.042 (3)	0.0103 (17)	0.0131 (19)	0.013 (2)
N7B	0.062 (3)	0.068 (3)	0.040 (3)	0.025 (3)	0.006 (2)	0.023 (3)
Zn	0.0331 (3)	0.0369 (3)	0.0277 (3)	0.0079 (2)	0.0052 (2)	0.0137 (2)
Br1	0.0391 (3)	0.0392 (3)	0.0574 (4)	0.0062 (2)	0.0161 (2)	0.0187 (3)
Br2	0.0535 (4)	0.0593 (4)	0.0712 (5)	0.0088 (3)	0.0129 (3)	0.0451 (4)
O1W	0.152 (6)	0.104 (5)	0.063 (4)	0.078 (4)	0.028 (4)	0.046 (3)

Geometric parameters (Å, °)

C1A—N6A	1.338 (7)	C1B—C5B	1.460 (7)
C1A—C2A	1.388 (7)	C2B—N7B	1.322 (7)
C1A—C5A	1.466 (7)	C2B—H2B	0.9300
C2A—N7A	1.330 (7)	C3B—N7B	1.324 (8)
C2A—H2A	0.9300	C3B—C4B	1.382 (9)
C3A—N7A	1.335 (8)	C3B—H3B	0.9300
C3A—C4A	1.381 (8)	C4B—N6B	1.340 (7)
C3A—H3A	0.9300	C4B—H4B	0.9300
C4A—N6A	1.329 (7)	C5B—N1B	1.313 (7)
C4A—H4A	0.9300	C5B—N5B	1.366 (6)
C5A—N1A	1.310 (7)	C6B—N2B	1.339 (7)
C5A—N5A	1.372 (6)	C6B—N5B	1.341 (6)
C6A—N3A	1.330 (6)	C6B—N3B	1.342 (6)
C6A—N2A	1.337 (6)	C7B—N4B	1.305 (6)
C6A—N5A	1.339 (6)	C7B—N3B	1.379 (7)
C7A—N4A	1.315 (7)	C7B—C8B	1.482 (7)
C7A—N3A	1.390 (7)	C8B—H8D	0.9600
C7A—C8A	1.487 (7)	C8B—H8E	0.9600
C8A—H8A	0.9600	C8B—H8F	0.9600
C8A—H8B	0.9600	N1B—N2B	1.381 (6)
C8A—H8C	0.9600	N2B—Zn	2.018 (4)
N1A—N2A	1.371 (6)	N3B—H3NB	0.85 (2)
N2A—H2NA	0.84 (2)	N4B—N5B	1.382 (6)
N3A—Zn	2.059 (4)	Zn—Br2	2.3581 (9)
N4A—N5A	1.384 (6)	Zn—Br1	2.4017 (11)
C1B—N6B	1.330 (6)	O1W—H1W	1.0251
C1B—C2B	1.381 (8)	O1W—H2W	0.9795
N6A—C1A—C2A	122.7 (5)	N7B—C2B—H2B	118.7
N6A—C1A—C5A	117.0 (4)	C1B—C2B—H2B	118.7
C2A—C1A—C5A	120.3 (5)	N7B—C3B—C4B	123.3 (5)

N7A—C2A—C1A	121.4 (5)	N7B—C3B—H3B	118.4
N7A—C2A—H2A	119.3	C4B—C3B—H3B	118.4
C1A—C2A—H2A	119.3	N6B—C4B—C3B	121.1 (5)
N7A—C3A—C4A	121.7 (5)	N6B—C4B—H4B	119.5
N7A—C3A—H3A	119.2	C3B—C4B—H4B	119.5
C4A—C3A—H3A	119.2	N1B—C5B—N5B	108.6 (4)
N6A—C4A—C3A	123.0 (6)	N1B—C5B—C1B	123.8 (5)
N6A—C4A—H4A	118.5	N5B—C5B—C1B	127.5 (4)
C3A—C4A—H4A	118.5	N2B—C6B—N5B	110.8 (4)
N1A—C5A—N5A	110.0 (4)	N2B—C6B—N3B	143.1 (5)
N1A—C5A—C1A	122.7 (4)	N5B—C6B—N3B	106.1 (4)
N5A—C5A—C1A	127.1 (5)	N4B—C7B—N3B	113.8 (4)
N3A—C6A—N2A	143.3 (5)	N4B—C7B—C8B	124.0 (5)
N3A—C6A—N5A	110.0 (4)	N3B—C7B—C8B	122.2 (5)
N2A—C6A—N5A	106.7 (4)	C7B—C8B—H8D	109.5
N4A—C7A—N3A	115.8 (4)	C7B—C8B—H8E	109.5
N4A—C7A—C8A	121.6 (5)	H8D—C8B—H8E	109.5
N3A—C7A—C8A	122.7 (5)	C7B—C8B—H8F	109.5
C7A—C8A—H8A	109.5	H8D—C8B—H8F	109.5
C7A—C8A—H8B	109.5	H8E—C8B—H8F	109.5
H8A—C8A—H8B	109.5	C5B—N1B—N2B	109.4 (4)
C7A—C8A—H8C	109.5	C6B—N2B—N1B	105.0 (4)
H8A—C8A—H8C	109.5	C6B—N2B—Zn	139.0 (3)
H8B—C8A—H8C	109.5	N1B—N2B—Zn	115.6 (3)
C5A—N1A—N2A	105.5 (4)	C6B—N3B—C7B	105.6 (4)
C6A—N2A—N1A	110.4 (4)	C6B—N3B—H3NB	128 (4)
C6A—N2A—H2NA	125 (4)	C7B—N3B—H3NB	125 (4)
N1A—N2A—H2NA	124 (4)	C7B—N4B—N5B	101.7 (4)
C6A—N3A—C7A	102.1 (4)	C6B—N5B—C5B	106.2 (4)
C6A—N3A—Zn	131.9 (4)	C6B—N5B—N4B	112.9 (4)
C7A—N3A—Zn	124.5 (3)	C5B—N5B—N4B	140.8 (4)
C7A—N4A—N5A	101.0 (4)	C1B—N6B—C4B	115.7 (5)
C6A—N5A—C5A	107.4 (4)	C2B—N7B—C3B	115.2 (6)
C6A—N5A—N4A	111.0 (4)	N2B—Zn—N3A	105.76 (17)
C5A—N5A—N4A	141.5 (4)	N2B—Zn—Br2	106.45 (13)
C4A—N6A—C1A	114.9 (5)	N3A—Zn—Br2	118.70 (12)
C2A—N7A—C3A	116.3 (5)	N2B—Zn—Br1	109.44 (14)
N6B—C1B—C2B	122.1 (5)	N3A—Zn—Br1	102.56 (12)
N6B—C1B—C5B	115.0 (5)	Br2—Zn—Br1	113.50 (4)
C2B—C1B—C5B	122.9 (5)	H1W—O1W—H2W	107.6
N7B—C2B—C1B	122.6 (6)		
N6A—C1A—C2A—N7A	-3.1 (8)	N6B—C1B—C2B—N7B	4.8 (10)
C5A—C1A—C2A—N7A	174.1 (5)	C5B—C1B—C2B—N7B	-175.6 (6)
N7A—C3A—C4A—N6A	-3.0 (9)	N7B—C3B—C4B—N6B	-0.2 (10)
N6A—C1A—C5A—N1A	173.9 (5)	N6B—C1B—C5B—N1B	-0.6 (7)
C2A—C1A—C5A—N1A	-3.5 (7)	C2B—C1B—C5B—N1B	179.8 (5)
N6A—C1A—C5A—N5A	-1.2 (7)	N6B—C1B—C5B—N5B	-178.4 (5)

C2A—C1A—C5A—N5A	-178.6 (5)	C2B—C1B—C5B—N5B	2.0 (8)
N5A—C5A—N1A—N2A	-0.3 (5)	N5B—C5B—N1B—N2B	1.5 (6)
C1A—C5A—N1A—N2A	-176.1 (4)	C1B—C5B—N1B—N2B	-176.7 (4)
N3A—C6A—N2A—N1A	178.4 (6)	N5B—C6B—N2B—N1B	-0.9 (6)
N5A—C6A—N2A—N1A	-0.9 (6)	N3B—C6B—N2B—N1B	176.8 (7)
C5A—N1A—N2A—C6A	0.7 (6)	N5B—C6B—N2B—Zn	172.4 (4)
N2A—C6A—N3A—C7A	-178.7 (7)	N3B—C6B—N2B—Zn	-9.9 (12)
N5A—C6A—N3A—C7A	0.6 (5)	C5B—N1B—N2B—C6B	-0.4 (6)
N2A—C6A—N3A—Zn	-12.6 (10)	C5B—N1B—N2B—Zn	-175.5 (3)
N5A—C6A—N3A—Zn	166.7 (3)	N2B—C6B—N3B—C7B	-177.2 (7)
N4A—C7A—N3A—C6A	-0.4 (6)	N5B—C6B—N3B—C7B	0.5 (5)
C8A—C7A—N3A—C6A	178.6 (5)	N4B—C7B—N3B—C6B	-0.9 (6)
N4A—C7A—N3A—Zn	-168.0 (4)	C8B—C7B—N3B—C6B	178.7 (5)
C8A—C7A—N3A—Zn	11.1 (7)	N3B—C7B—N4B—N5B	0.8 (5)
N3A—C7A—N4A—N5A	0.1 (6)	C8B—C7B—N4B—N5B	-178.7 (5)
C8A—C7A—N4A—N5A	-178.9 (5)	N2B—C6B—N5B—C5B	1.8 (6)
N3A—C6A—N5A—C5A	-178.9 (4)	N3B—C6B—N5B—C5B	-176.8 (4)
N2A—C6A—N5A—C5A	0.7 (5)	N2B—C6B—N5B—N4B	178.5 (4)
N3A—C6A—N5A—N4A	-0.6 (5)	N3B—C6B—N5B—N4B	-0.1 (6)
N2A—C6A—N5A—N4A	179.0 (4)	N1B—C5B—N5B—C6B	-2.0 (5)
N1A—C5A—N5A—C6A	-0.3 (5)	C1B—C5B—N5B—C6B	176.1 (5)
C1A—C5A—N5A—C6A	175.3 (5)	N1B—C5B—N5B—N4B	-177.2 (5)
N1A—C5A—N5A—N4A	-177.7 (5)	C1B—C5B—N5B—N4B	0.9 (10)
C1A—C5A—N5A—N4A	-2.1 (9)	C7B—N4B—N5B—C6B	-0.4 (5)
C7A—N4A—N5A—C6A	0.3 (5)	C7B—N4B—N5B—C5B	174.6 (6)
C7A—N4A—N5A—C5A	177.6 (6)	C2B—C1B—N6B—C4B	-2.5 (8)
C3A—C4A—N6A—C1A	2.0 (8)	C5B—C1B—N6B—C4B	177.8 (5)
C2A—C1A—N6A—C4A	1.0 (7)	C3B—C4B—N6B—C1B	0.3 (8)
C5A—C1A—N6A—C4A	-176.3 (5)	C1B—C2B—N7B—C3B	-4.3 (10)
C1A—C2A—N7A—C3A	2.1 (8)	C4B—C3B—N7B—C2B	2.1 (10)
C4A—C3A—N7A—C2A	0.8 (8)		

Hydrogen-bond geometry (\AA , $^\circ$)

$D-H\cdots A$	$D-H$	$H\cdots A$	$D\cdots A$	$D-H\cdots A$
C2A—H2A \cdots Br1 ⁱ	0.93	3.13	3.995 (6)	155
N2A—H2NA \cdots N1B	0.84 (2)	2.09 (4)	2.786 (6)	139 (5)
N2A—H2NA \cdots N6B	0.84 (2)	2.39 (4)	3.126 (6)	145 (5)
C2B—H2B \cdots N4B	0.93	2.62	3.276 (7)	129
C4B—H4B \cdots Br1 ⁱ	0.93	2.86	3.791 (6)	176
N3B—H3NB \cdots O1W	0.85 (2)	1.85 (3)	2.669 (6)	163 (6)
O1W—H1W \cdots Br1 ⁱⁱ	1.03	2.39	3.375 (6)	162
O1W—H2W \cdots N7A ⁱⁱⁱ	0.98	2.03	2.901 (7)	148

Symmetry codes: (i) $-x+1, -y, -z+1$; (ii) $-x, -y+1, -z+1$; (iii) $x-1, y+1, z$.